FoT25: Studies of Embedded Weapons Bays – Summary Report

TORSTEN BERGLIND, SHIA-HUI PENG AND LARS TYSELL

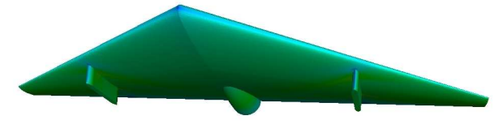

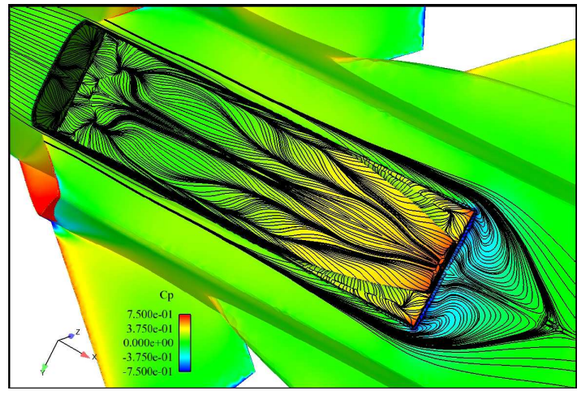

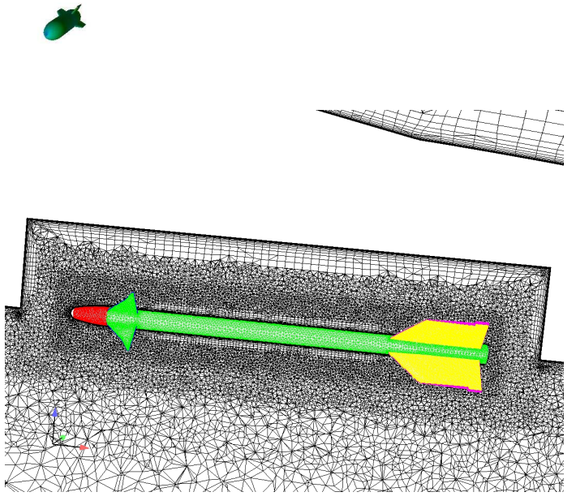

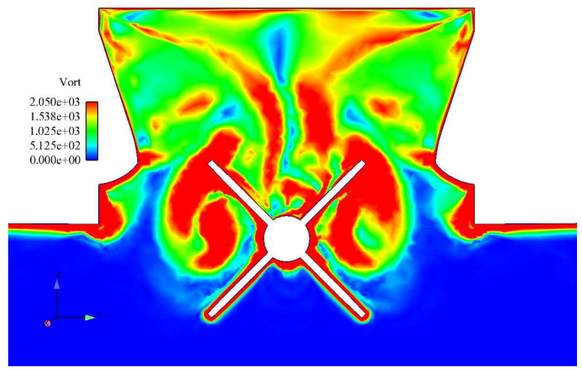

FOI
Defence Research Agency
Defence & Security,
Systems and Technology
SE-164 90 Stockholm

Phone: +46 8 555 030 00
Fax: +46 8 555 031 00

www.foi.se

FOI-R--2775--SE Technical report
ISSN 1650-1942 June 2009

Defence & Security, Systems and Technology

Torsten Berglind, Shia-Hui Peng and Lars Tysell

FoT25: Studies of Embedded Weapons Bays – Summary Report

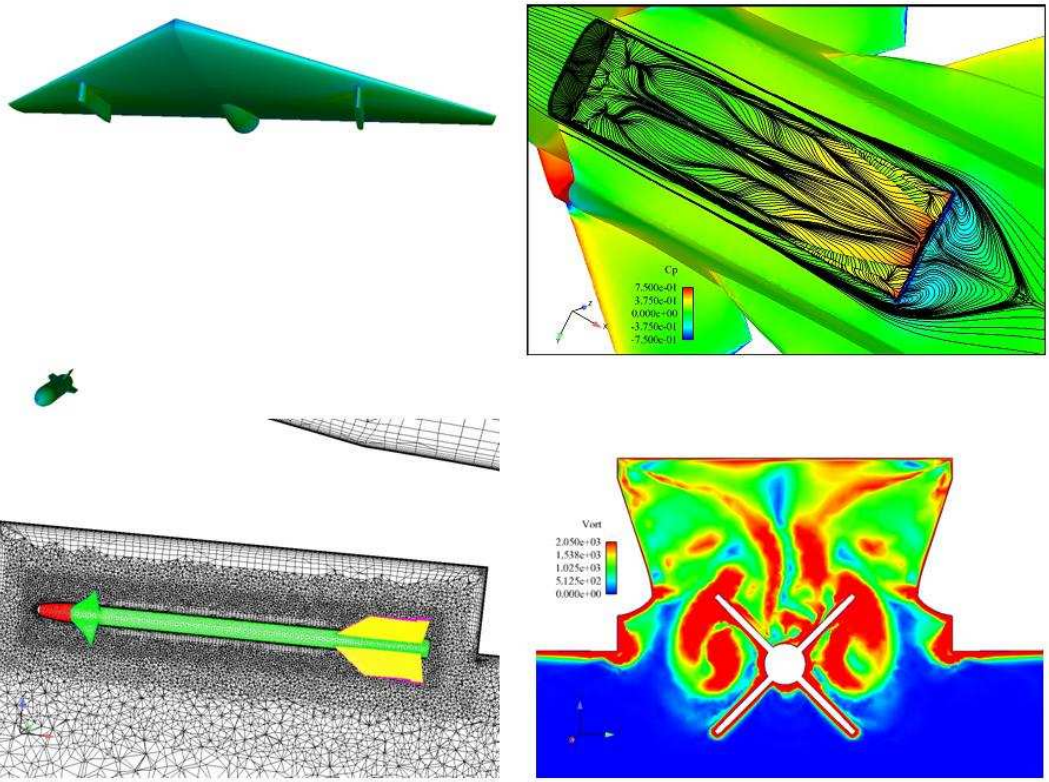

Titel	FoT25: Studiier av inre vapenutrymme – sammanfattningsrapport
Title	FoT25: Studies of Embedded Weapons Bays – Summary Report

Rapportnr/Report no	FOI-R--2775--SE
Rapporttyp Report Type	Teknisk rapport Technical Report
Sidor/Pages	32 p
Månad/Month	Juni/June
Utgivningsår/Year	2009
ISSN	ISSN 1650-1942
Kund/Customer	FMV
Kompetenskloss	19 Flygteknik, rymd och robotar
Extra kompetenskloss	
Projektnr/Project no	E61351
Godkänd av/Approved by	Maria Sjöblom

FOI, Totalförsvarets Forskningsinstitut
Avdelningen för Försvars- och säkerhetssystem

164 90 Stockholm

FOI, Swedish Defence Research Agency

SE-164 90 Stockholm

Sammanfattning

Denna rapport sammanfattar arbetet och slutsatserna av FoT25-projektet “Studier av inre vapenutrymme”. Inre vapenutrymmen förbättrar smygegenskaper och kan medge ökad manövrerbarhet och räckvidd för framtida flygfarkoster. Huvudsyftet med detta projekt har varit att utveckla kunskap om hur instationär strömning runt vapenschakt påverkar flygprestanda, väggarna i vapenschaktet och separationsbanorna för vapenlasten. Numeriska simuleringar av strömning runt framtidskonceptet FS2020 med vapenschakt har genomförts. Den numeriska upplösningen i beräkningsrummet är fokuserad till området i och runt vapenschaktet. Simuleringarna av instationär strömning har huvudsakligen gjorts med DES och hybrid RANS-LES-metoder. Inledningsvis undersöktes inverkan av nätfinhet och olika fysikaliska modeller. En kil i framkanten av vapenschaktet dämpade fluktuationerna inuti vapenschaktet väsentligt. För att kunna prediktera separationsbanor, kopplades kvasistationära strömningsberäkningar till en flygmekanisk modell. Ett integrerat system för simulering av vapenseparation med strömningslösaren Edge har utvecklats. Den relativa rörelsen mellan flygplan och last avbildas med en sekvens av deformerade och lokalt omgenererade nät. Den flygmekaniska modellen består av ekvationssystemet för stelkroppsrörelse som löses med ett 5:e ordningens Runge-Kutta-schema. För att validera implementationen av systemet för flerkroppsrörelser beräknades ett AGARD-fall för separation av extern last. En fenförsedd missil separerades från en generisk vinge-sting-pylon-konfiguration med hjälp av en ERU (Eject Release Unit). Beräknad separationsbana och attitydvinklar stämmer bra med experiment.

Nyckelord: lastfällning, vapenschakt, instationär strömning, stelkroppsmodell, hybrid RANS-LES modell, kavitetsströmning.

Summary

This report summarizes the efforts and conclusions made in the FoT25-project “Studies of Embedded weapons bays”. Employing internally embedded weapons bays improves stealth properties and may increase manoeuvre ability and range for future air vehicles. The main purpose of the project has been to gain knowledge about the impact of unsteady flow around weapons bays on flight performance, on the cavity walls and on store separation trajectories. Numerical simulations of flow around the FS2020 military aircraft model with internally embedded weapons bays are carried out. The spatial resolution in the modelling is focused inside and around the weapons bay. Emphasis has been on unsteady simulations using the DES and a hybrid RANS-LES modelling approach. Initial investigations of spatial resolution and various flow physics models were carried out. The effect of a wedge along the upstream edge of the weapons bay damped the pressure fluctuations substantially. In order be able to predict trajectories, quasi-steady aerodynamics is coupled to flight mechanics. An integrated system for store separation computations with the flow solver Edge has been developed. The relative movement between the aircraft and the store is mapped by a sequence of deformed and locally remeshed grids. The flight mechanics model consists of the equations for rigid body motion solved by a fifth order Runge-Kutta scheme. In order to validate the implementation, an AGARD-test case for external store separation was computed. A finned missile is separated from a generic wing-sting-pylon configuration with use of an ERU (Eject Release Unit). The computed trajectories and attitudes agree well with experiment.

Keywords: store separation, weapons bays, unsteady flow, rigid body-model, hybrid RANS-LES model, cavity flow.

Contents

1 Introduction

This report summarizes the efforts and conclusions made in the FoT25-project “Studies of Embedded Weapons Bays”. Detailed descriptions of the technical activities can be found in the FOI Technical Reports [1, 2, 3 and 4]. The purpose of this report is to give a brief overview of what has been done and to describe the context that has motivated the activities. Another purpose is to explain the long term perspective of this research.

Future military manned and unmanned air vehicles will be provided with weapons bays to improve the aircraft aerodynamic performance and to achieve low observable characteristics. External weapons carriages may contribute as much as 30% of the total drag of an air vehicle, and in addition, substantially increase the radar signature of the aircraft. The main purpose of this project has been to gain knowledge about the impact of unsteady flow around weapons bays on flight performance, on cavity walls and on store separation trajectories.

An important objective is to explore the unsteady flow features in the presence of an open weapons bay. Numerical simulations of flow around the FS2020 military aircraft model, a Saab future concept for manned fighter aircraft, with internally embedded weapons bays are carried out. The main motive is better understanding of the aerodynamic effects around internal weapons carriage. This in turn will serve as a knowledge base to pursue well-controlled flow and aerodynamic conditions prior to the deployment of in-flight store separation.

Along with some steady RANS computations, the emphasis is placed on unsteady simulations using the DES and a hybrid RANS-LES modelling approach. Also the effect on the flow with a missile placed in the weapons bay was investigated.

The numerical analysis has been focused on the flow inside and around the weapons bay embedded in the aircraft fuselage. Prior to the deployment of store separation with open doors, the weapons-bay flow is unsteady by nature, due to the mixing layer that impacts on the aft wall of the bay cavity and entailing extensive pressure oscillations inside the weapons bay. The resolved instantaneous flow features, as well as some time-averaged (mean) flow properties, have been explored. It is shown that the presence of an open weapons-bay implies increased drag and a reduced lift for the aircraft model, but both are very limited, as compared to the bay-closed configuration. In addition, the pressure gradient over the weapons-bay floor, as well as the pressure fluctuations on the bay-cavity surface, has also been investigated. These are factors closely related to the aerodynamic forces acting on the store and on the structure of the weapons bay. Also investigations of flows with a missile placed in the weapons bay opened prior to the deployment of store separation have been performed. On the basis of the present results, an outlook is given on some aspects for future investigation of the aircraft model with store in the weapons bay in terms of flow control.

The other part of the project has been aiming to develop a system for computations of trajectories for separated stores, involving the motion of complex geometry, three-dimensional bodies embedded in external, temporally and spatially evolving flows. Numerical modelling of these phenomena requires coupled CFD and flight mechanics computations, a general system for gridding bodies in relative movement, interpolation of solutions from previous grids, etc. This part has implied development of new functionalities connected to our general purpose flow solver Edge [5]. Some of these parts have been integrated into Edge whereas other parts are separate programs linked to Edge via scripts.

In the present work, quasi-steady approach is used to model the motion of separating an external store relative to its parent aircraft, using steady Euler flow computations, adding effects of aerodynamic damping. The implementation of a 6DOF (six degree of freedom) flight mechanics model for a rigid body and its coupling to CFD is developed [2]. The strategy for modelling moving bodies is to use an ALE (Arbitrary Lagrangian-Eulerian) methodology on unstructured grids [6-8]. The grid movement is modelled by a combination of grid stretching and remeshing, interpolating preceding solutions from previous grid levels onto successive grids.

Analysis of store separation trajectories for external loads can usually be carried out successfully using the assumption of quasi-steady flow [9]. If the unsteady effects of the flow on the trajectories are significant, wind tunnel tests are of limited use since it’s not possible to simultaneously capture all dimensionless parameters characterising the physical processes. A long term goal is to be able to predict trajectories for unsteady flow conditions simulating three-dimensional, time dependent, compressible flows about moving bodies. Flight

clearance procedures for unsteady flow conditions have to be extremely conservative since the trajectories will not be repeatable.

2 Flow computations around weapons bays

2.1 Computational Set-up

One of the main purposes of this work was to investigate the aerodynamic effect of weapons bay on a military aircraft. The FS2020 model has been used in the computations, being exposed to a free stream with Mach number $M_\infty = 0.9$, Reynolds number $Re = 16 \cdot 10^6$, at angle of attack of $\alpha = 9^o$.

The FS2020 model is a SAAB future concept for manned fighter aircraft. The two main features of FS2020 are supercruise and internal weapons carriage systems, see Figure 2.1. The FS2020 aircraft model consists of two weapons bays embedded in the fuselage. The front bay, located between the air-intake ducts, is designed for light weapons and the back bay for heavy weapons between the main landing gears. In accordance with the suggestion by SAAB, only the effect of the front weapons bay, without modelling the bay doors, has been investigated.

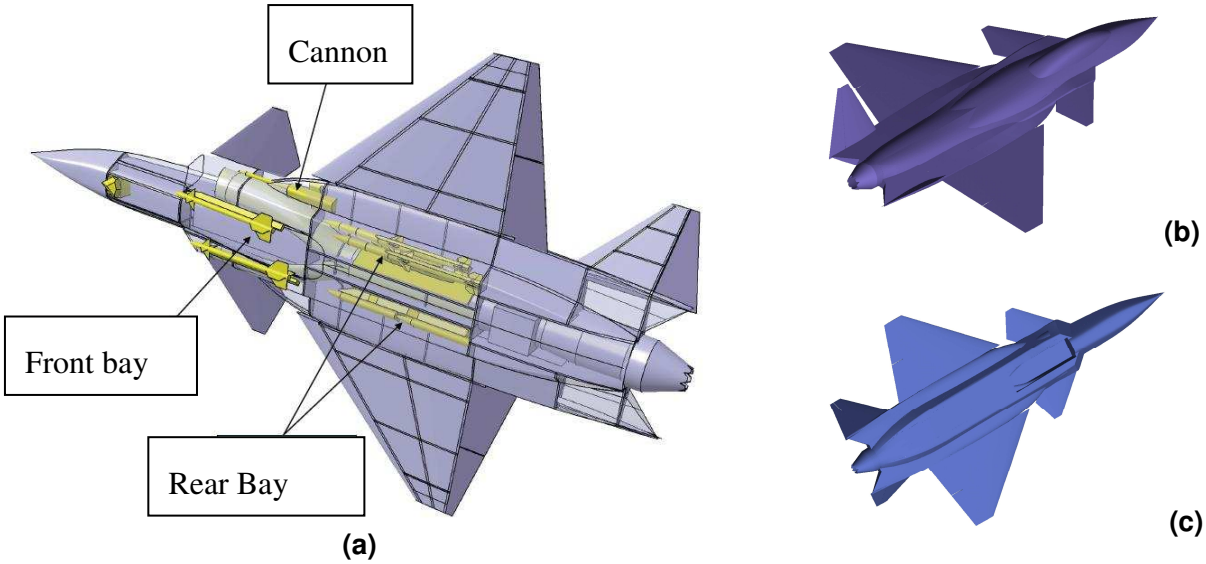

Figure 2.1 Schematic of the weapons bay of the FS2020 aircraft configuration. (a). Location of weapons bay; (b). Top view of clean FS2020 model; (c) Bottom view of clean FS2020 model.

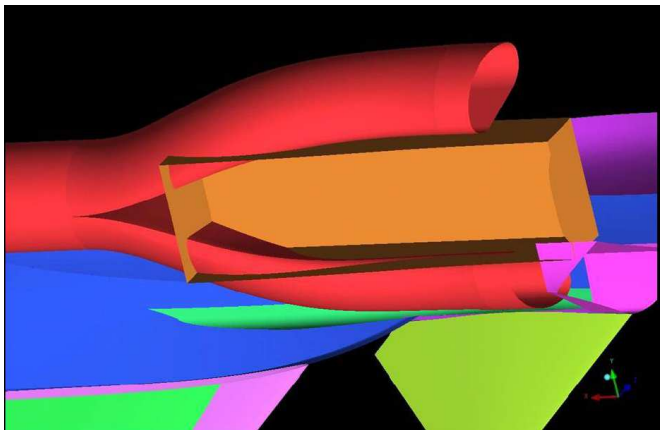

Figure 2.2: Intersection of the front weapons bay with the duct of air intake (flow is from right to left).

As illustrated in Figure 2.2, the air-intake duct wall forms a part of the side walls of the weapons bay cutting through the rear corner. In the computation, the flow through the air-intake ducts is not simulated, but the duct inflow section is taken as an outflow boundary with given mass flow rate.

Initially, a half-body model was employed for both RANS and hybrid RANS-LES modelling. The purpose was to highlight the general weapons bay flow features and its potential aerodynamic effects on the aircraft performance. The use of the half-model in the computation was motivated in order to save the computational cost and to perform some effective numerical analysis on the effect of grid resolution, due to relatively heavy unsteady computations with the DES and hybrid RANS-LES models. The computation started with a baseline mesh which contains about 2.8 million and 2.24 million nodes, respectively, for the open and closed weapons bay cases. With the baseline mesh, it was noticed that, the generated grid resolution is reasonable to resolve the mixing layer over the bay opening and the flow in the bay cavity, but the grid resolution over the canard, wing and fuselage is somewhat too coarse. A refined grid was thus generated, with about 5.08 million and 4.53 million nodes, respectively, for the bay-open and bay-closed cases. With both the baseline and the refined grids, about 0.55 million nodes have been allocated in the bay cavity. In Figure 2.3 the meshing on the top surface of aircraft is illustrated for both the baseline and the refined grid. As shown, grid refinement has occurred mainly on the fuselage surface and the leading edges of the wing and canard.

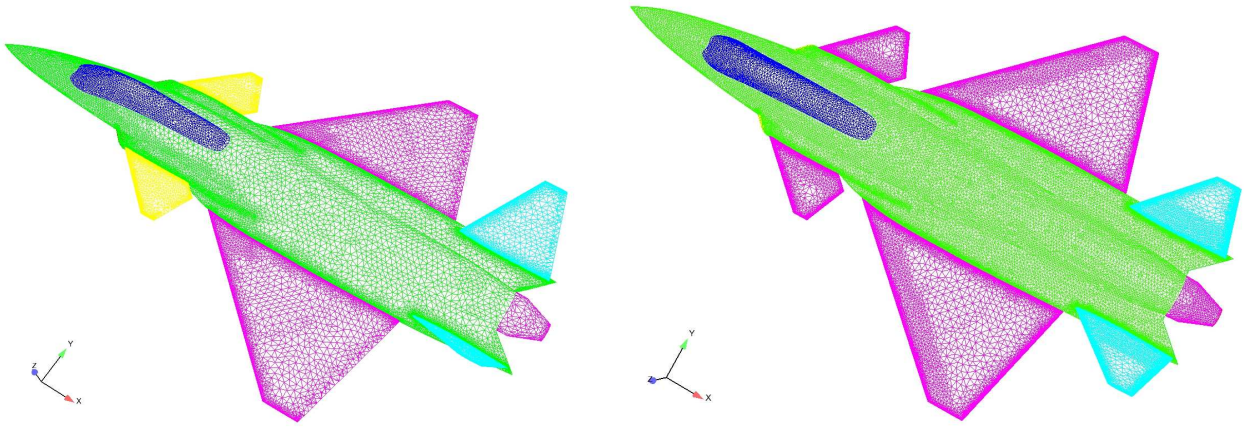

Figure 2.3 Surface mesh on the top surface of aircraft model. Left: baseline grid; Right: Refined grid.

A cutting at the half-cavity length ($L_c/2$) is further presented in Figure 2.4, to highlight the grid resolution in and around the bay cavity. Note that, with both grids, the emphasis of the grid resolution has been placed on the region around the weapons bay, especially in the vicinity of the upstream boundary layer and the subsequent free shear layer over the bay cavity, which has been regarded as being the major ingredient to characterize the flow features of the weapons-bay flow.

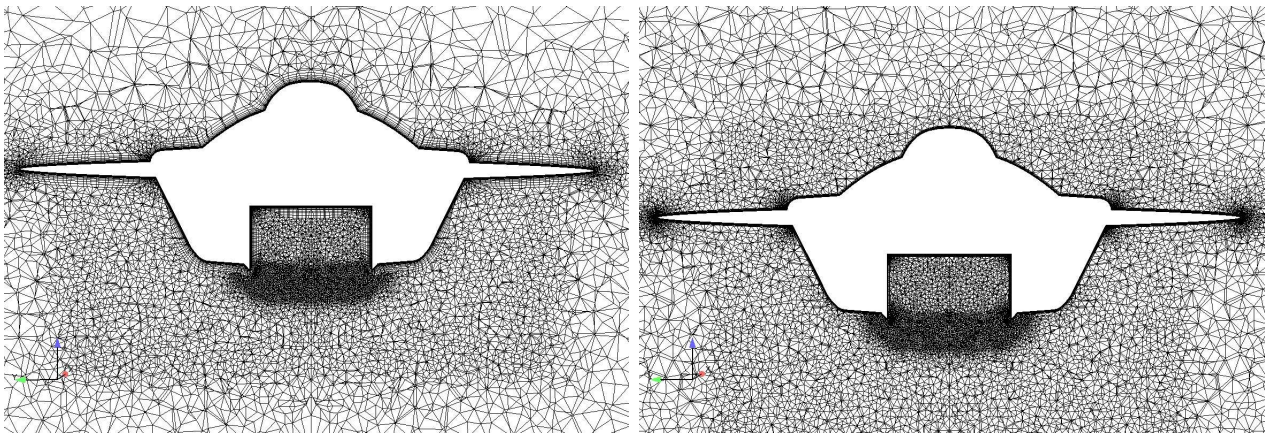

Figure 2.4 A Schematic of the baseline and refined grids cut at the half-cavity length. Left: baseline grid; Right: Refined grid.

2.2 Numerical computations

The numerical simulation has been carried out using the FOI unstructured Navier-Stokes solver EDGE, which is a node-based Euler/Navier-Stokes solver for the compressible flow equation system using finite volume method [5]. The details of the computation can be referred to the work presented in Refs [3, 4], here a brief summary is given below.

In table 1 and table 2 the integrated forces computed on the baseline and the refined grid are shown. It is clear that the presence of an open weapons bay implies an increased drag and a reduced lift, albeit both are quite limited, as compared to the bay-closed configuration.

Cases	**Closed (S-A RANS)**	**Open (S-A RANS)**	**Closed (S-A DES)**	**Open (S-A DES)**	**Open (HYB0)**
C_D	0.0988	0.1008	0.0984	0.1014	0.1037
C_L	0.5884	0.5868	0.5854	0.5839	0.5880
C_M	-0.0752	-0.0742	-0.0684	-0.0699	-0.0725

Table 1: Integrated forces computed with the baseline grid (half-model configuration).

Cases	**Closed-new (S-A RANS)**	**Open-new (S-A RANS)**	**Open (HYB0)**
C_D	0.0969	0.0981	0.0987
C_L	0.5931	0.5901	0.5733
C_M	-0.0687	-0.0686	-0.0702

Table 2: Integrated forces computed with the refined grid (half-model configuration).

In Figure 2.5a, an example is illustrated for the resolved instantaneous flow motion with the HYB0 simulation. A close view is given in Figure 2.5b for the instantaneous pressure distribution on the cavity surface, where the insert indicates the instantaneous pressure distribution along the centerline of the cavity floor. As shown, an adverse pressure gradient arises over the cavity, which may instantaneously raise to a rather large level. This is not desirable for store separation, since it may cause nose-up pitching moment on the store.

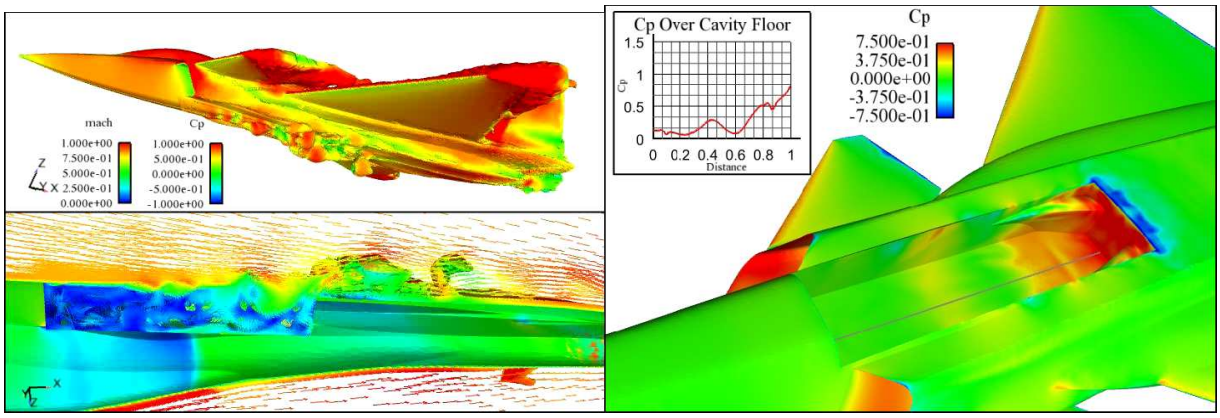

a. Instantaneous vortex motion over and in the bay cavity. b. Instantaneous surface pressure.

Figure 2.5: Resolved instantaneous vortex motion (Ω = 1000) over the weapons bay. The solid surfaces are coloured with the pressure coefficient C_p and the iso surfaces are couloured by with Mach number.

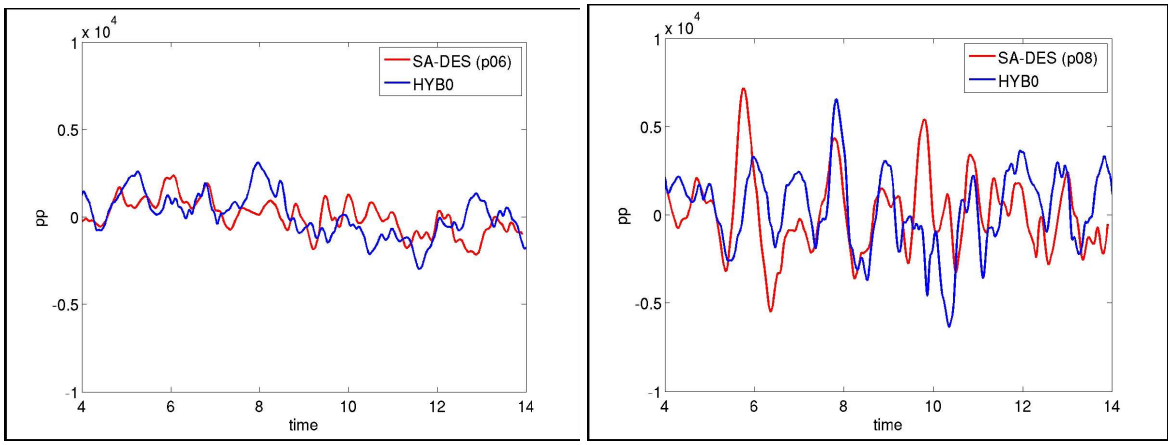

a. Point p06 (0.15 L_c from the cavity fron wall) b. Point p08 (0.35 L_c from the cavity fron wall)

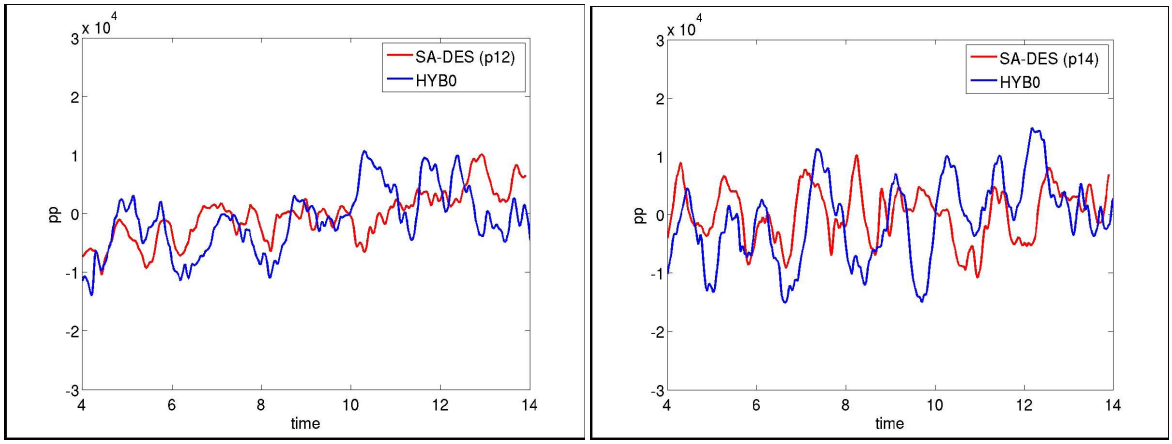

c. Point p12 (0.75 L_c from the cavity fron wall) d. Point p14 (0.95 L_c from the cavity fron wall)

Figure 2,6: Pressure fluctuations with time, S-A DES and HYB0 modelling with the baseline grid.

With unsteady analysis, it is possible to explore the instantaneous force acting on the weapons bay structure by sampling the surface pressure fluctuations in and around the bay cavity. In Figure 2.6, the pressure fluctuations

recorded on the cavity floor along the centreline at locations p06, p08, p12 and p14 are presented, which are located from the cavity front wall at a distance of, respectively, 0.15 L_c, 0.35 L_c, 0.75 L_c and 0.95 L_c. As seen, the amplitude of pressure fluctuations increases along the cavity floor, as the flow is approaching the cavity rear wall (from p06 to p14), due to the impact of the mixing layer on the aft wall. With the present free stream flow condition and the cavity aspect ratio, namely, M_∞ = 0.9 and a length-to-depth ratio of L_c/D_c = 5.75, the flow over the weapons bay cavity should present resemblance with an open-cavity flows. This would suggest that the mixing layer may bridge over the cavity opening and, consequently, self-sustaining pressure oscillations may generate high-amplitude tonal modes. There are two phenomena characterizing the feedback loop: the mixing layer vortices moving downstream at a velocity proportional to U_∞ and the pressure waves travelling upstream inside the cavity at the speed of sound. The predicted fluctuating intensity of the surface pressure in the cavity is thus closely related to the mixing layer impinging on the cavity aft wall and of the resulting flow motion in the cavity. Figure 2.7 presents further the SPL(Sound Pressure Level) at the four locations described above. As shown, the spectra do not present significant tonal peaks. Both the DES and the HYB0 models have produced similar broadband SPL levels, ranging from about 50 dB to 150 dB for a range of frequencies less than 2000 Hz. The magnitude of SPL is generally similar to previous studies with similar flow conditions, the absence of sensible tonal modes in the spectra is however different. As mentioned, there are two factors that may have diminished the spectral tones of the pressure oscillations, namely, the angle of attack and the blockage of the air-intake duct on the rear part of the bay cavity.

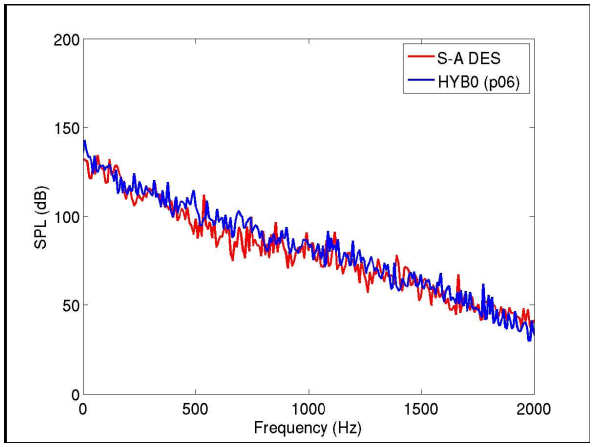

a. Point p06

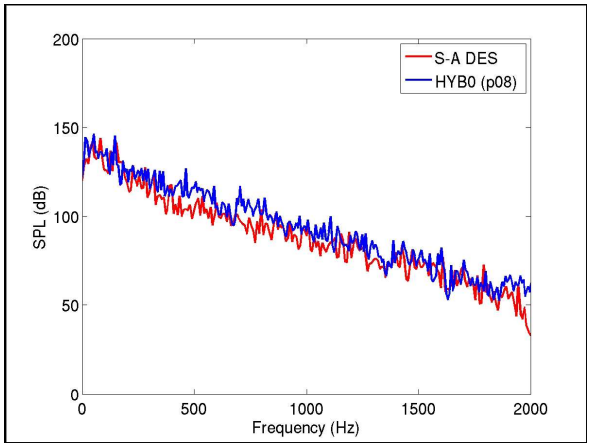

b. Point p08

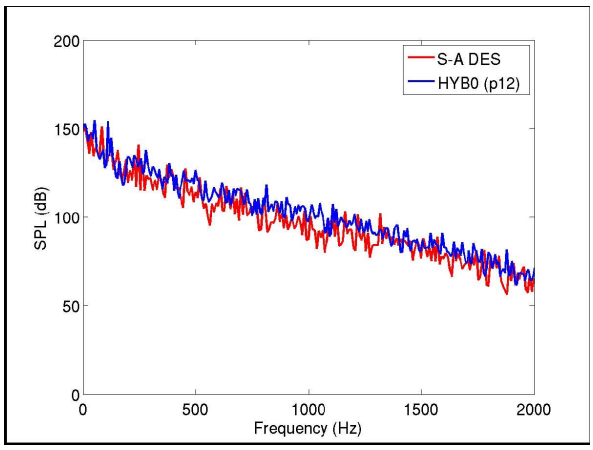

c. Point p12.

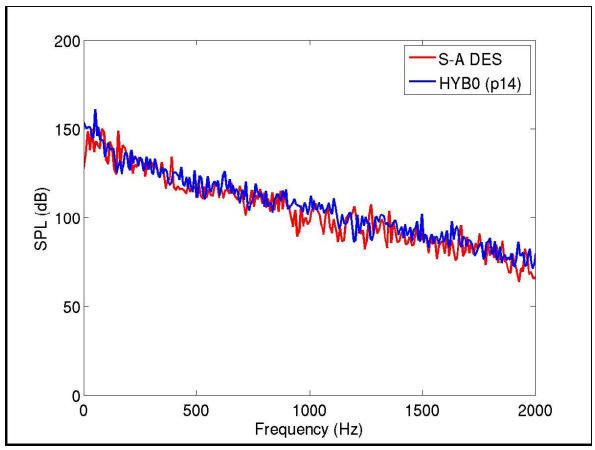

d. Point p14

Figure 2.7: Sound pressure level (SPL) on the cavity floor at locations p06, p08, p12 and p14. Results have been computed with the baseline grid.

In the second part of numerical analysis of weapons bay flow features, a missile model (AIM9L) has been placed in the bay cavity for the computation with the same free stream flow conditions. Two store locations of the missile

have been considered, namely, at the mid-height of the bay cavity (**store-in**) and at the bay opening (**store-out**). The latter position mimics the location prior to the deployment of store separation. In these analyses, the whole-body configuration has been considered. Due to large requirement of computing costs, nonetheless, only one preliminary unsteady computation has been conducted using the hybrid RANS-LES HYB0 model. The other computations have been undertaken with the S-A RANS model. Two additional RANS computations have also been carried out with a spoiler (a wedge) attached on the edge of the cavity front wall, with the purpose to control the mixing layer over the bay opening. This has been done for both the store-in and store-out cases, and is termed **store-in+Sp** and **store-out+Sp**, repectively. The mesh has been generated based on the refined grid for the half-model configuration, particularly, for the grid over the upstream boundary layer of the bay cavity and for the grid over the mixing layer and inside the bay cavity. Nonetheless, some nodes over the top surface of the aircraft have been saved, as compared with the grid for the half-body configuration.

Figure 2.8 presents a few examples to show the grid resolution for both store-out and store-in cases, which has been cut respectively at the mid-section of the cavity width and at a location over the rear fins of the missile. As shown, the resolution is about the same for both cases, but the prismatic layers over the bay floor are somewhat different for different store locations.

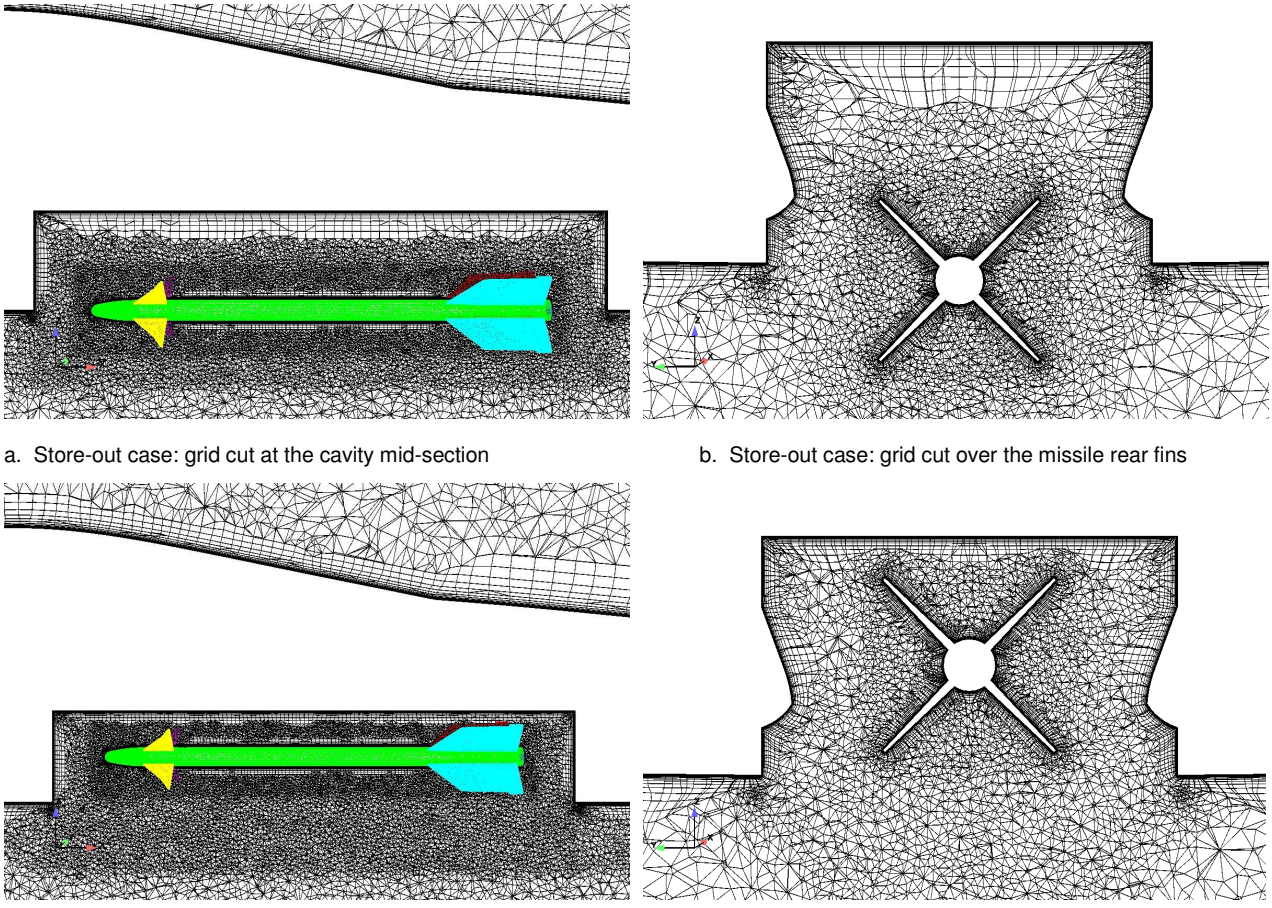

a. Store-out case: grid cut at the cavity mid-section

b. Store-out case: grid cut over the missile rear fins

c. Store-in case: grid cut at the cavity mid-section

d. Store-in case: grid cut over the missile rear fins

Figure 2.8: Illustration of grid resolution in the cavity for two different store locations.

In order to reduce the possible nose-up pitching moment that may potentially be induced by the adverse pressure gradient, a spoiler is employed and is attached on the edge of the bay-cavity front wall. It is expected that the spoiler will alter and re-direct the incoming mixing layer, alleviating its impact on the aft wall. Computations with the spoiler have also been performed for both store-in and store-out cases. Figure 2.9 illustrates the spoiler (coloured with red on at the leading edge of the bay cavity), where a grid cut at the cavity mid-section is also presented for the store-out case.

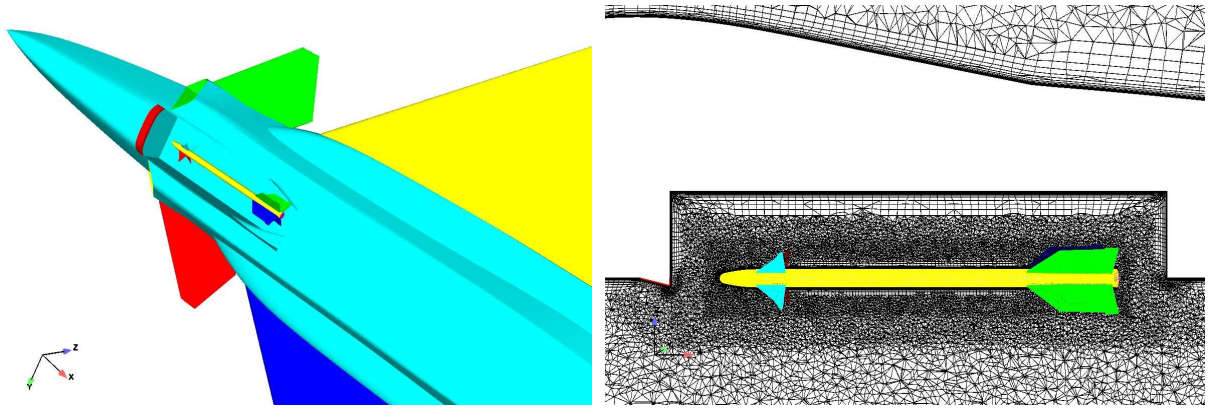

Figure 2.8: Bay cavity with a spoiler attached at the edge of the front wall to control the incoming mixing layer.

All the cases have been computed with the S-A RANS model. For the store-out case, a preliminary computation has also been carried out using the HYB0 model. As an example, Figure 2.9 illustrates the resolved vortex motion over the bay opening and in the bay cavity. It is noted that, with no store, the mixing layer is often broken down at about the half-cavity length after emanating from the cavity leading edge [10,11]. The presence of a store in the opening has largely altered the flow feature, by which the impact on the cavity aft wall is alleviated.

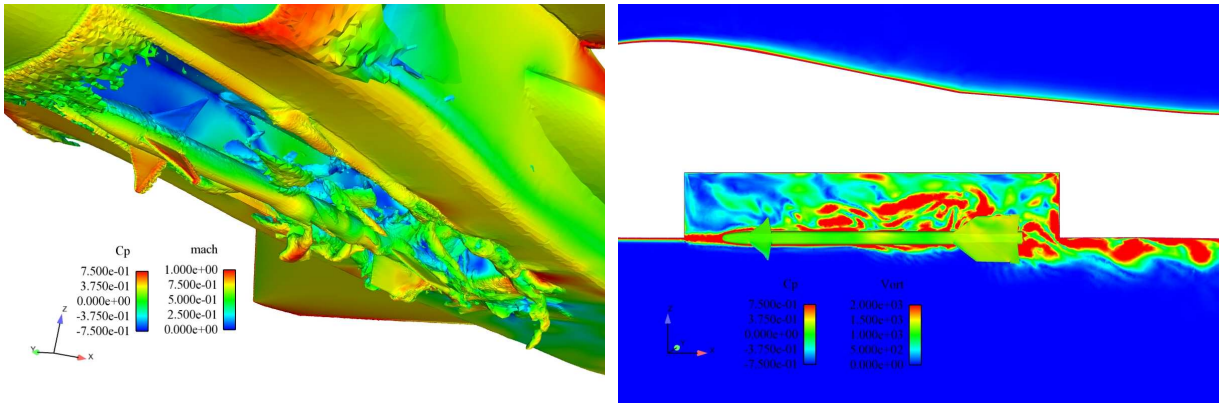

Figure 2.9: Illustration of the resolved vortex motion for the store-out case with the HYB0 model.

This can be further observed from the plotting for the mean flow streamlines, as shown in Figure 2.10. With no store, the mixing layer impacts on the cavity aft wall and causing a recirculation flow inside the bay cavity. With the store in the bay and below the opening, the impact of mixing layer is slightly altered, the reverse flow on the bay floor becomes more intensified in the presence of the missile inside the bay. Moving the missile to the bay opening, the store is directly exposed to the mixing layer and has alleviated its impact on the cavity aft wall. The flow motion inside the bay cavity has been somewhat relaxed. The center of the recirculation flow in the bay is shifted close the store surface, which often indicates a region with lower pressure.

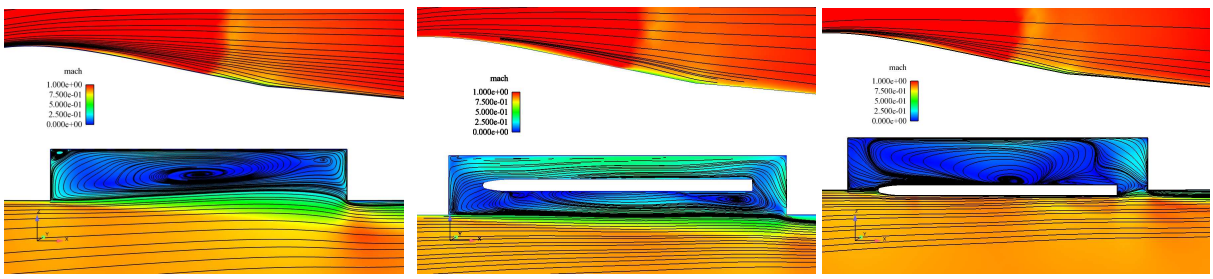

Figure 2.10: Mean flow streamline plotted on the mid-section of the cavity width. Left: with no store; Middle: with store in bay (store-in case). Left: with store on the bay opening (store-out case);

In Figure 2.11, the effect of the spoiler on the mean flow feature is highlighted, taking the store-out case as an example. As expected, the presence of the spoiler has re-directed the incoming boundary layer, shifting mixing layer somewhat away from bay opening where the missile is located. The mixing layer does not impact on the aft wall. Consequently, the recirculation flow inside the bay cavity becomes less extensive and its center shifts toward the bay floor. This is clearly demonstrated by a close view of the flow around the missile head with and without the spoiler, as shown in Figure 2.11.

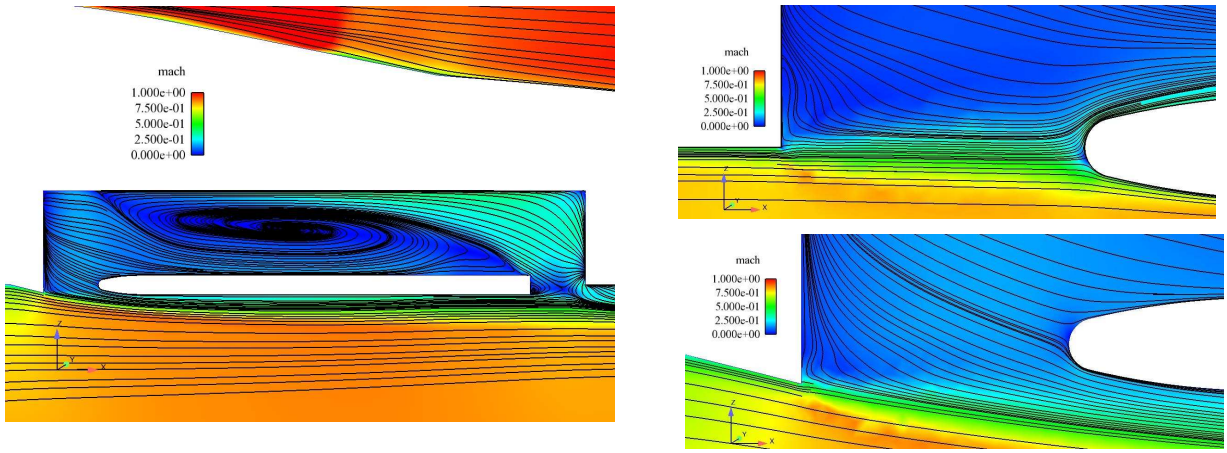

Figure 2.11: Mean flow streamline plotted on the mid-section of the cavity width with the store placed on the bay opening. Right-upper: Close view for Store-out case (with no spoiler); Left-lower: Close view for Store-out+Sp case (with spoiler).

The flow feature in and around the bay cavity, with the store placed at different locations, has insignificant effect on the aerodynamic force for the aircraft, as shown in Table 4. These values are very similar to the results obtained with the half-body configuration (see Tables 1 and 2). Nonetheless, these flow features have changed the aerodynamic force acting on the store, as shown in tables 3 and 4.

Case	**Store-out (HYB0)**	**Store-out (SA RANS)**	**Store-out+SP (SA RANS)**	**Store-in (SA RANS)**	**Store-in+SP (SA-RANS)**
C_D	0.0949	0.1092	0.1100	0.1097	0.1100
C_L	0.5421	0.5953	0.5872	0.5909	0.5883
C_M	-0.0625	-0.0699	-0.0686	-0.0697	-0.0686

Table 3 Integrated forces on the aircraft (whole-body configuration)

The introduction of the spoiler has, however, changed significantly the aerodynamic forces acting on the store, as shown in tables 5. Without the spoiler for the store-out case, both HYB0 and RANS computations have claimed undesired nose-up pitching moment of the missile. The use of the spoiler (store-out+SP) has turned the pitching moment to the opposite direction in association with the flow features presented above. The flow control for store separation from an embedded weapons bay is an interesting topic. This should be further investigated in terms of, for example, the optimization of flow-control device and active flow control during the deployment of store separation, where the aerodynamic forces on the store can be taken as the objective functions.

Case	**Store-out (HYB0)**	**Store-out (SA RANS)**	**Store-out+SP (SA RANS)**	**Store-in (SA RANS)**	**Store-in+SP (SA-RANS)**
CM	7.4819	7.9606	-15.788	-10.7832	-19.4335
CY	0.0755	0.0715	-0.8658	2.5606	-1.0737
CR	0.0530	0.0342	0.1210	0.1987	-0.1606

Table 4 Predicted moments for the missile, where CM indicates the pitching moment, CY is the yawing moment and CR is the rolling moment.

3 Trajectory computations

3.1 Overview

Development of capability to compute trajectories requires grid generation package for general movements, flight mechanics model and flow solver for unsteady aerodynamics.

From an initial flow solution, integrated forces of the moving object are computed and passed on to the flight mechanics model. A new position is computed and the coordinates of the new boundary points are sent to the grid deformation module. After the grid is adapted to the new position, the grid quality is checked. If the grid quality is OK, volumes and surfaces of the modified grid cells are recomputed and the flow solution is computed. If the grid quality is not OK, the flow solver is stopped and a new grid is computed. A new dual grid is computed by the pre-processor.

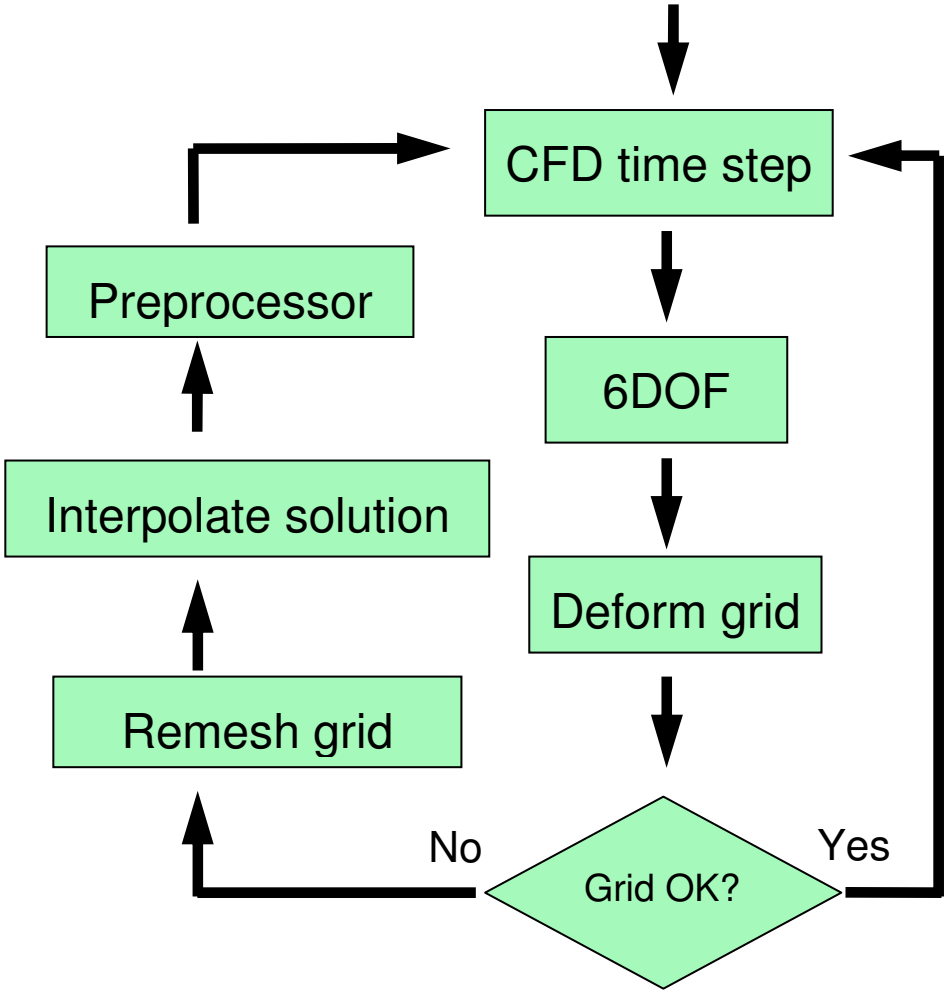

Figure 3.1 Flow chart of the trajectory computations coupled to the remeshing modules.

3.2 Flight Mechanics Model

The flight mechanics model is a rigid body model. The Euler's equations for classical mechanics [12, 13] can be rewritten as a system of four first order differential equations in time,

$$\begin{aligned}
&\ddot{\vec{r}}_C = \frac{\vec{F}}{m} \\
&\dot{\vec{r}}_C(t) = \int_{t_0}^{t} \frac{\vec{F}}{m} dt + \dot{\vec{r}}_C(t_0) \\
&\vec{L}'_C = \dot{\vec{\omega}}' I'_C + \vec{\omega}' \times (\vec{\omega}' I'_C) \\
&\dot{\vec{\Omega}}' = \vec{\omega}'
\end{aligned} \tag{3-1}$$

where $\vec{F}$ is the resultant force on the body, m is the mass, $\vec{r}_C$ is the position vector to the mass centre, $\vec{L}_C$ is the r relative to the mass centre, $\vec{\omega}$ is the angular velocity, and I_C is the inertia tensor with respect to the mass centre, is the velocity and position of the mass centre, t is the time at the new time step and t_0 is the time at the previous tin rotation vector and ´ denotes the moving reference frame. This system of equations can be rewritten as,

$$\begin{aligned}
&\vec{q} = \begin{pmatrix} \dot{\vec{r}}_C \\ \vec{r}_C \\ \vec{\omega}' \\ \vec{\Omega}' \end{pmatrix} \\
&\dot{\vec{q}} = \vec{f}(\vec{q})
\end{aligned} \tag{3-2}$$

, where $\vec{f}$ is the right hand side of the corresponding equations. Integration of equation (3-2) in time is done with a fifth order accurate Runge-Kutta method RKF45 (Runge-Kutta-Fehlberg).

Quasi-steady computations imply that the flow at each moment of the movement is considered as steady. In order to take the body's own movement into account, aerodynamic damping coefficients are applied [14]. The aerodynamic damping moment $\vec{M}'_d$ is computed as,

$$\vec{M}'_d = \begin{pmatrix} M'_{Ld} \\ M'_{Md} \\ M'_{Gd} \end{pmatrix}$$

$$\begin{aligned}
M'_{Ld} &= C_{lp} P b_r \frac{1}{2V_r} q_{dyn_r} S_r c_r \\
M'_{Md} &= C_{mq} Q c_r \frac{1}{2V_r} q_{dyn_r} S_r c_r \\
M'_{Gd} &= C_{nr} R c_r \frac{1}{2V_r} q_{dyn_r} S_r c_r
\end{aligned} \tag{3-3}$$

where M'_{Ld}, M'_{Md} and M'_{Gd} are components of the aerodynamic damping moment, C_{lp}, C_{mq} and C_{nr} are aerodynamic damping coefficients, P,Q, and R are the rotation rates, V_r is the velocity of the moving body, q_{dyn_r}

is the dynamic pressure on the moving body, S_r is reference area, c_r is reference length and and b_r is reference span. The values of the aerodynamic damping coefficients C_{lp}, C_{mq} and C_{nr} are always negative.

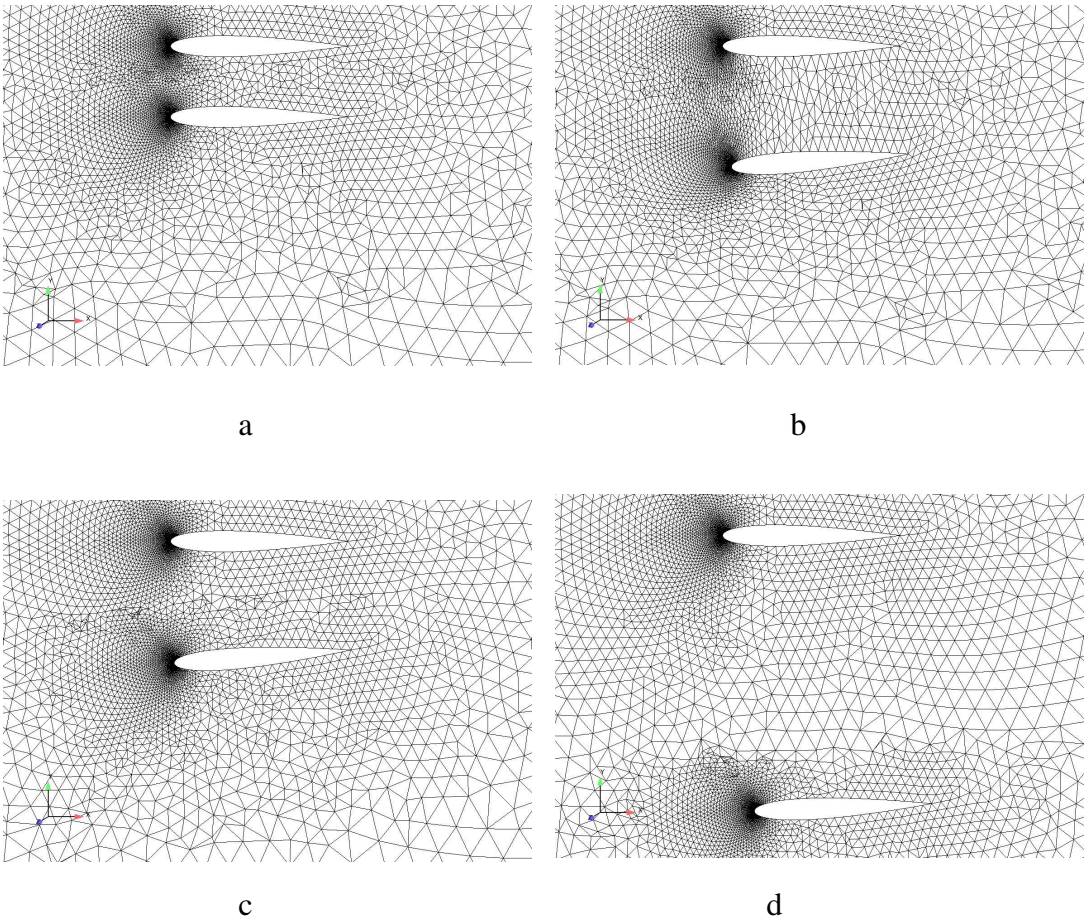

Figure 3.2 Illustration of the gridding process: a. Initial grid, b. deformed grid at its final position, c. Remeshed grid in the same position, d. Grid with the moving object in a position further down.

3.3 Grid Generation

Describing a general movement is of course challenging for grid generation systems. The philosophy for our approach is to, as far as possible; describe the movement with grid deformation, i.e. to move the position of the nodes, such that the new grid conforms to the updated boundaries of the moving object. FOI has experiences with this technique from computations with prescribed motion, aeroelastic computations and aerodynamic shape optimisation. This capability is built into the flow solver Edge. A trajectory computation implies that this technique will be extended to its utmost limit. As the object is moved further and further away from its original position, the quality of the grid will inevitably decrease until it finally is too poor to be used. In some cases volumes of elements will be negative and in other cases the grid will simply be too sparse. A special routine is developed in order to decide whether the grid is sufficiently good or not.

In Figure 3.2 two wing profiles are separated from one another. From the initial position in Figure 3.2a the grid is stretched until it reaches the position in Figure 3.2b. The grid quality routine announces that the grid cannot be stretched further and therefore exits the Edge computation. A new grid is generated with the local remeshing program, Figure 3.2c. This process continues until the computations reach its final position, Figure 3.2d.

The local remeshing procedure starts from a reference grid around the main object and another grid around the moving object, see Figure 3.3a. The grid around the moving object is cut by one or several inner boxes, see Figure 3.3b. The grid between the innermost parts of the inner boxes and the body will remain fixed relative to the moving object, regardless of the position of the moving object. The purpose of the inner boxes is to enable positioning the moving object close enough to the reference object. An outer box marks the outer boundary for which the grid will be modified.

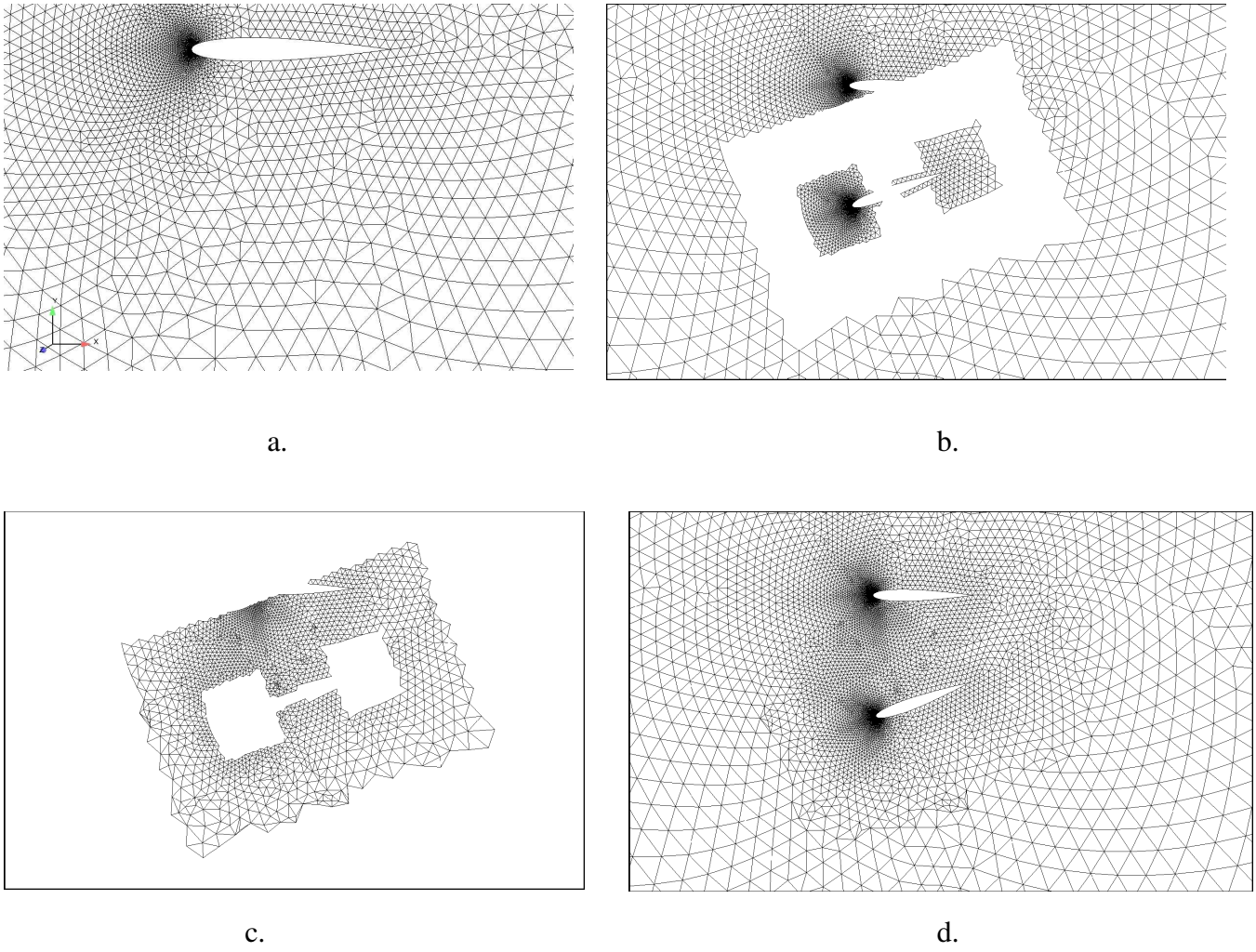

Figure 3.3 Illustration of local remeshing: a. Initial grid, b. Cut a hole in the reference grid, c. Filling the hole with grid, d. Merged grid

The outer boundary may intersect the reference object. The domain between the union of the inner boxes and the outer box is gridded with an advancing front method [1], Figure 3.3c. The different parts of the grid are merged to a complete grid, figure 3.3d. The advantage with this technique is that the original grid is modified locally, thereby retaining the major features of the original grid. CFD solutions are always, to some extent, grid dependent and it is therefore a good idea to change the original grid as little as possible.

.

3.4 Store separation from a generic wing-sting-pylon configuration

In order to validate the implementation of a flight mechanics model in Edge, an AGARD test case carried out at AEDCs (Arnold Engineering Development Centre) 4-Foot Transonic Aerodynamic Wind Tunnel (4T) is selected, see reference [9]. A generic finned-store shape and a clipped delta wing with a 45 degree leading edge sweep were the primary test objects, see Figure 3.4. The full-scale store model length is 3.018 m.

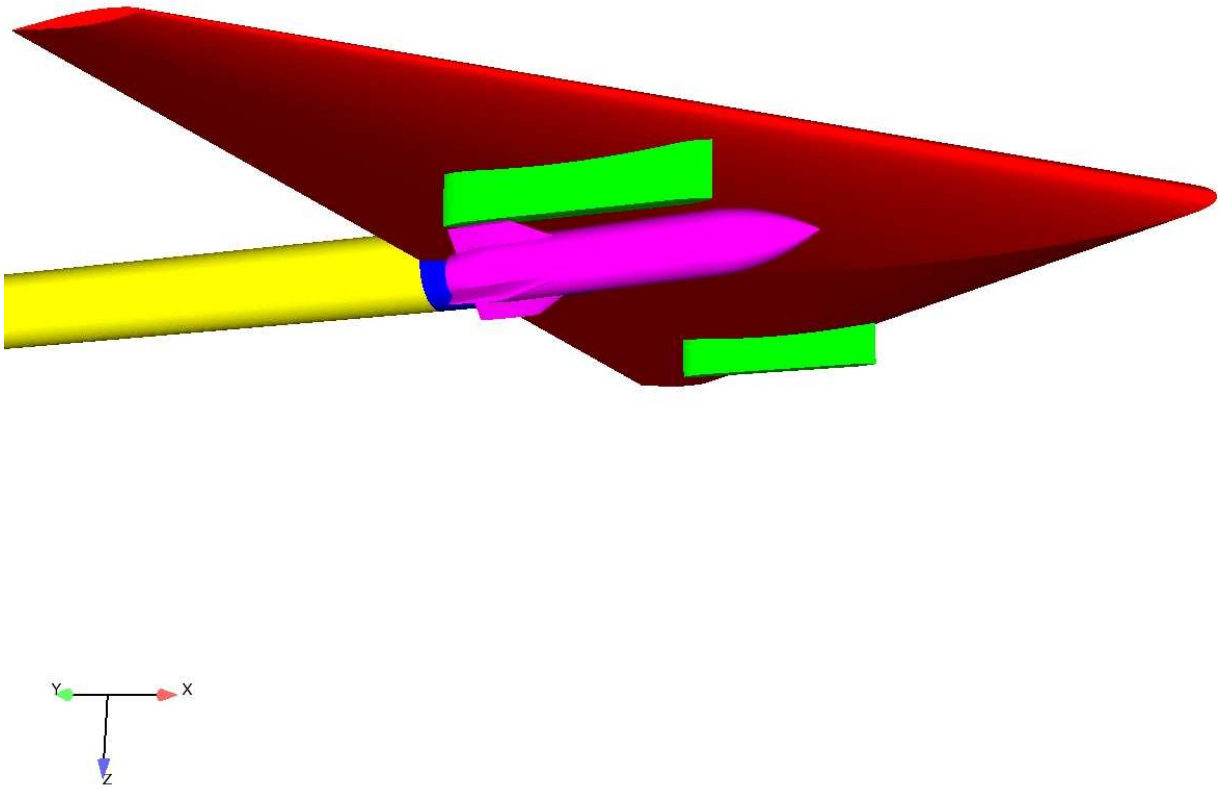

Figure 3.4 Start position for the finned store in computations.

The wind tunnel tests are carried out with CTS (Captive Trajectory System) technique. The store is attached to a separate sting that is moved with computer controlled motors. An online 6-DOF computer program solves equations of motion which gives next position of initial conditions for each step. The temporal steps to update the store positions are 0.0002 seconds in pseudo time, falling store real time.

The available data corresponds to the store mounted on the right side of the wing. The flow case is hence asymmetric and therefore a full model is required for the computations. The ERU (Ejection Release Unit) consists in this case of two pistons with the ejector stroke length 0.10 m which are released simultaneously. The forward ejection location is 1.24 m and the aft ejector location is positioned 1.75 m aft of the store nose. The forward ejector force is 10675.7 N and the aft ejector force is 42702.9N, both constant in time. A model of the ERU itself is at the current stage not implemented in the code.

The rig was positioned such that the store at carriage nearly touched the left or right pylons in the initial position, as required to initiate a trajectory. Since the primary goal was to validate the coupling of the flight mechanics model to CFD, it was decided to omit the part of the separation where the pistons are in physical contact with the store. The moment when the contact between the pistons and the store cease to occur, appears approximately 55 ms after it has left the original position. The computations are therefore started at the subsequent temporal measurement station, 60 ms after the store has left the original position, see Figure 3.4. Thereby the ERU only influences the initial condition of the computations.

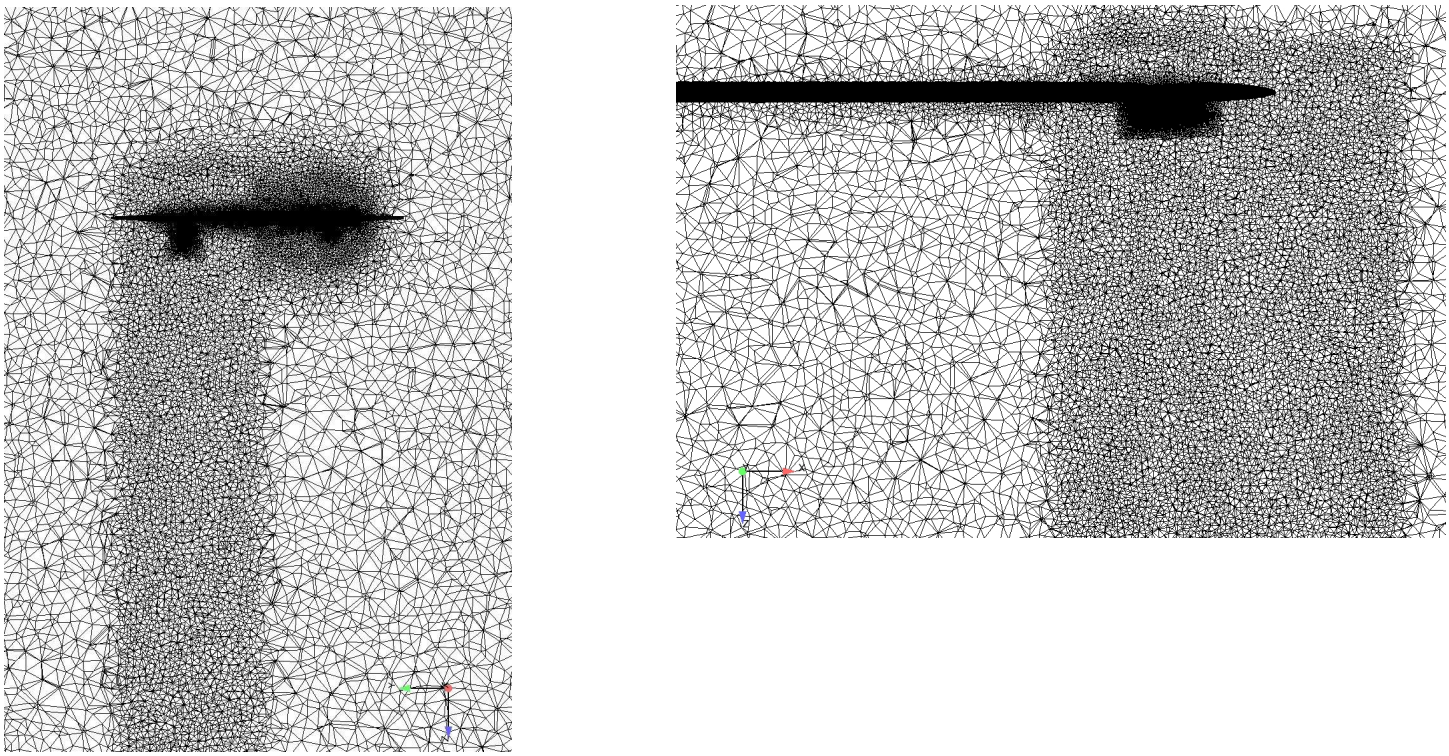

Figure 3.5 Grid cuts through the computational grid seen from in front of the aircraft. The number of nodes is 1765565 grid points.

Two unstructured tetrahedral grids were generated around the aircraft with $5.7 \cdot 10^6$ nodes and around the missile with $0.20 \cdot 10^6$ nodes. This grid was coarsened outside the vicinity of the aircraft and away from the trajectory path to a grid with $1.8 \cdot 10^6$ nodes, Figure 3.5. The grids with both the aircraft and the missile in various positions are then generated by a merge of the two grids using the local remeshing routine, Figure 3.8.

First a steady computation is performed for the missile in its initial position. Quasi-steady computations are started and the grid is stretched every time step to conform to new positions. The grid quality is checked for each new grid and if it is not satisfactory, the flow computations are stopped. A new grid is generated with the local remeshing routine and the flow solution on the previous grid is interpolated onto the new grid. The computations continue until the specified number of iterations is computed. The whole procedure is managed by a shell-script.

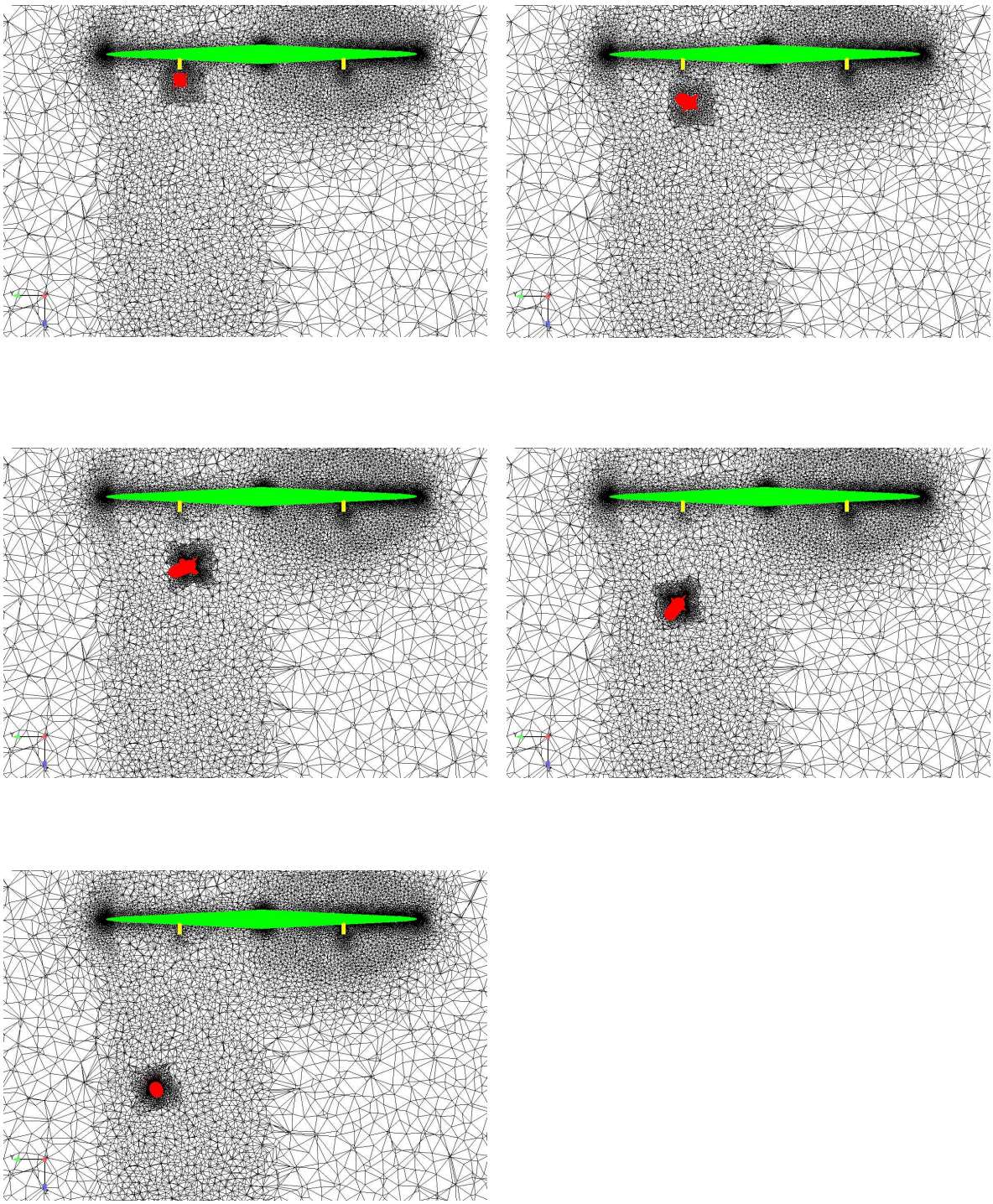

Figure 3.6 A grid cut through the computational grid seen from in front of the aircraft. The merged grid with .the missile at subsequent positions.

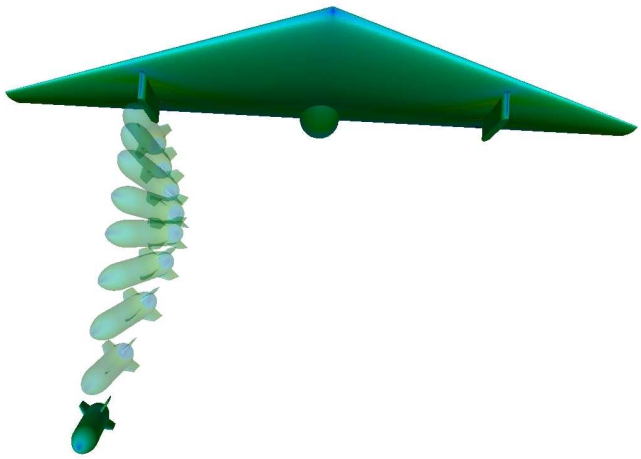

Figure 3.7 Mach number distribution for free stream Mach number M=0.95 and angle of attack 0°. The non transparent store is in the position after t=0.87 sec.

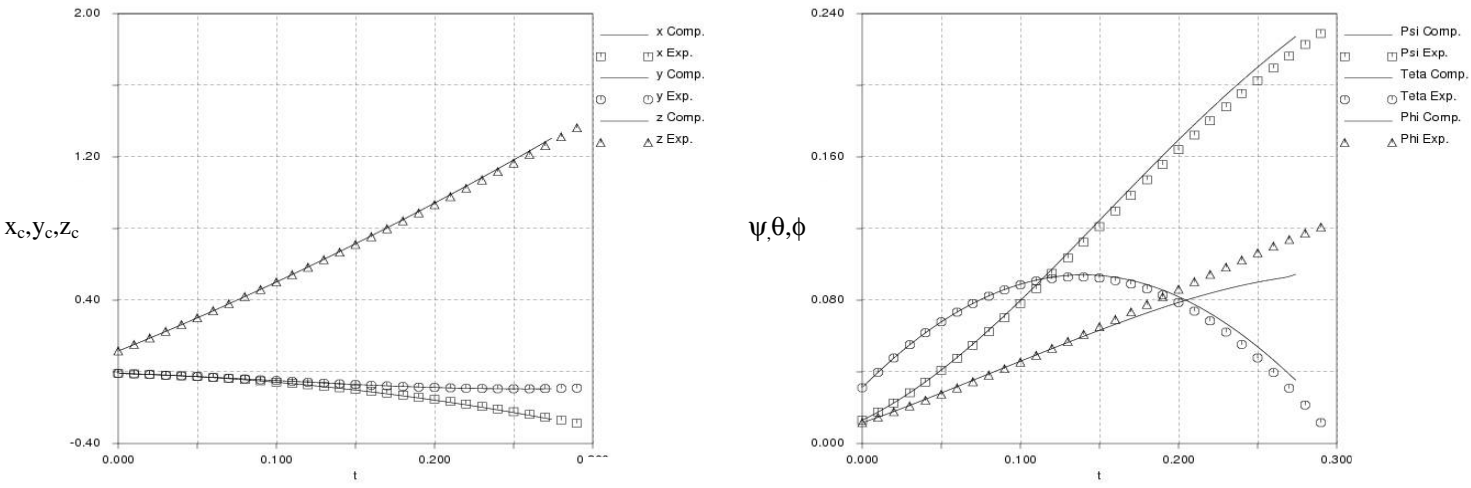

Figure 3.7 Trajectory and attitude for a quasi-steady Euler computation with Δt = 0.001 sec.

The results for Δt = 0.001 sec are plotted against experiments, see Figure 3.7. Good agreement is achieved for both the trajectory and attitude, except for the roll angle. The store separation scenario can be seen in Figure 3.6. A time step convergence study showed that the solution successively approaches the experimental values as the time step is decreased. There are therefore good reasons to believe that the result will improve further with a smaller time step. The reason for not carry out computations with a finer grid is that the flow solver code for

trajectory computations was parallelized shortly before the project ended. However, the agreement with experiments is almost as good as the reference computation in reference [9].

4 Conclusions and outlook

One of the main purposes with the computational analysis is to explore the potential aerodynamic effects on a military aircraft with an embedded weapons bay that is opened for the deployment of store separation. The accomplishment of the project will serve to bring a better understanding of the flow around and in a realistic weapons bay being exposed to practical flight conditions. Furthermore, by aerodynamic optimization and flow control, the work will be undertaken further for possible improvement of the weapons bay design with the purpose of suppressing the extensive pressure oscillations and providing the best condition prior to the deployment of store separation.

The computations have shown that the flow over the aircraft is, apart from some small regions with local flow separations, is characterized by boundary layers attached on the wall surface. The unsteady computations using DES and hybrid modelling have even predicted a slight flow separation at the canard and wing leading edges on the suction side, which is not produced by steady RANS computations. Moreover, a shock wave is identified from the computation on the inboard sections of the canard and the wing.

It is shown that turbulence energy is generated mainly in the bay-cavity, due to strong shear and flow deformation. The flow inside the cavity is characterized by three-dimensional motions, which are clearly indicated by DES and HYB0 modelling. As compared with bay-closed case, all the numerical computations with the weapons bay have indicated an increase of $1.25 - 3.1\%$ in the integrated drag and a reduction of $0.2 - 0.3\%$ in the lift of the aircraft model. Due probably to the penetration of the air-intake ducts in the bay cavity, the pressure oscillations predicted by both the HYB0 and DES models do not present any tonal modes, as produced in previous studies. The amplitude of the pressure oscillations are however declared at about the same level. Moreover, the computations have indicated an adverse pressure gradient existing in the stream-wise direction along the cavity floor. This adverse pressure gradient should be regulated when in-flight store separation is deployed.

With store (a missile) in the bay cavity at two different locations, the computation has shown that the integrated forces of the aircraft are insignificantly affected by the store location, in spite of the fact that the flow pattern is altered sensibly inside the bay. With the store placed in the bay, the mixing layer is only slightly disturbed and the reverse flow over the bay floor becomes relatively intensive. When the store is moved to the bay opening, the mixing layer is broken and the recirculation flow in the bay is weakened. The integrated force acting on the store is closely associated to the store location, however. At the bay opening, the store is subjected to an undesirable nose-up pitching moment, which can nevertheless be removed with the use of the spoiler. Comprehensive investigation of the flow control for store separation should be an interesting topic to serve improved design of embedded weapons bay.

An integrated system for numerical simulation of store separation for quasi-steady flow has been developed and validated. A six Degree of Freedom rigid body-model has been implemented in Edge, FOI's multipurpose flow solver. The grid is deformed in order to conform to the moving boundaries. The computations are coupled to grid generation modules to remesh the grid, if the grid deformation module fails to achieve sufficient grid quality. Typically 10-15 remeshings are required for a store separation trajectory.

Quasi-steady Euler calculations is carried out for an AGARD test-case, separation of a finned store from a wing-sting-pylon configuration. The computational results compares well with wind tunnel measurements, except some minor deviation of the roll angle. The effect of aerodynamic damping was small in this case. In the future, computations of store separation of unsteady flow will be compared with these results. This comparison is of special interest since wind tunnel measurements correspond to quasi-steady analysis and flight test corresponds to the unsteady analysis.

In the original project plan the final goal was to develop capability to do trajectory computations for Navier-Stokes computations. It was also planned to do some initial trajectory computations around the FS2020

configuration. However, the funding of the project was reduced substantially and it was therefore not possible to fulfill these goals.

In order to be able to do Navier-Stokes computations it remains to develop some new functionalities. A routine is needed to mark the nodes in the prismatic layer to avoid streching of the grid in the boundary layer region. Since grid deformation in trajectory computations contexts modifies the grid substantially, especially close to the store surface, it will be important to retain the grid intact in this sensitive region. In order to be be able to restart time accurate computations, routines for interpolation of the solution for two previous time levels needs to be developed. Time accurate computations also require fully coupled aerodynamics and flight mechanics calculations, i.e. grid deformations and flight mechanics calculations have to be carried out each subiteration.

The first steps towards a general system for coupling CFD and flight mechanics models have been developed. This new functionality enables computations of a new class of flow problems. Conceivable applications apart from store separation are pilot ejection and specific A/C manoeuvres dominated by non linear aerodynamics.

5 Acknowledgements

This work has been carried out with the support of the Swedish Defence Materiel Administration, FMV. Ingemar Persson at SAAB Aerosystems has been project leader for the FoT25-project: “Studies of Embedded Weapons Bays”. The authors would like to thank Ingemar Persson and Anders Lindberg at SAAB Aerosystems for interesting discussions and helpful suggestions. The authors also wish to acknowledge colleauges at FOI, Peter Eliasson for parallellising the routines for trajectory computations and for reviewing the implementation plan, Oskar Enoksson for writing the shell-scripts for trajectory computations and generation of movies, and finally Henrik Edefur for generating the CAD-file and the initial grid files for the AGARD test case.

6 References

[1] Tysell L., “Implementation of Local Remeshing Routines in Edge”, FOI-R-2550-SE, 2007.

[2] Berglind T. “Numerical Simulation of Store Separation for Quasi-Steady Flow”,. FOI-R-2761-SE, 2008.

[3] Peng S.-H., “Numerical Analysis of FS2020 Military Aircraft Model with Weapons Bay”, FOI-Memo-2489, FOI, 2008.

[4] Peng S.-H., “CFD Investigation of A Militart Aircraft Model with Enbedded Weapons Bay ”, FOI-R-2786 (in preparation), FOI, 2009.

[5] Eliasson P., “Edge, a Navier-Stokes Solver for Unstructured Grids”, Proceedings of Finite Volumes applications III, ISBN 1-9039-9634-1, pp. 527-534, 2002

[6] Baum J. D., Lou H. and Löhner R.,”A New ALE Adaptive Unstructured Methology for the Simulation of Moving Bodies”, AIAA 94-0414(1994).

[7] Lijewski L.and Suhs N.,“Time Accurate Computational Fluid Dynamics Approach to Transonic Store Separartion Trajectory Prediction”, Journal of Aircraft, Vol 31, No. 4, July-Aug. 1994.

[8] Coleman L., Jolly B., Chesser B.L. and Brock J., “Numerical Simulation of a Store Separation Event from an F15-E Aircraft”, AIAA 96-3385(1996).

[9] Fox J.H.,”Generic wing pylon, and moving finned store”, Arnold Engineering Development Center(AEDC), Arnold AFB, TN 37389-6001, USA.

[10] S.-H. Peng. Unsteady RANS simulation of turbulent cavity flow: Summary of 2D baseline computations. FOI-R-1915-SE, Systems Technology, Swedish Defence Research Agency, Stockholm, 2006.

[11] S.-H. Peng. Unsteady rans simulation of a turbulent flow over a weapon bay cavity. Scientific Report, FOI-R-1983-SE, FOI, Swedish Defence Research Agency, Stockholm, 2006.

[12] Goldstein H., “Classical Mechanics”, Addison-Wesley Publishing Company, Inc, 1950.

[13] Fox E. A., “Mechanics”, Harper and Row Publishers,1967.

[14] Persson I. and Lindberg A., “Transonic Store Separartion Studies on the SAAB Gripen Aircraft Using Computational Aerodynamics”, ICAS 2008-2.9.1, 2008.